

**Original Research Article****Optimal design of stand-alone photovoltaic system based on battery storage system: A case study of Borj Cedria in Tunisia**Safa Slouma<sup>1,2,\*</sup>, Wael Boulaares<sup>1,3</sup>, Somnath Maity<sup>4</sup>, Abdelmajid Jemni<sup>1</sup>, Souheil El Alimi<sup>1</sup><sup>1</sup> Thermal and Energy Systems Studies Laboratory (LESTE), LR99ES31, National Engineering School of Monastir (ENIM), Monastir University, Monastir 5000, Tunisia<sup>2</sup> National Institute of Applied Science and Technology (INSAT), University of Carthage, Tunis 1080, Tunisia<sup>3</sup> General Directorate of Technological Studies (DGET), sise à l'ISET de Radès, Radès Médina 2098, Tunisia<sup>4</sup> Department of Electrical Engineering, Rourkela National Institute of Technology, Rourkela, Odisha 769008, India\* **Corresponding author:** Safa Slouma, safa.slouma@enit.utm.tn

**Abstract:** This work dealt with the optimal design of a stand-alone photovoltaic system (SAPS) based on the battery storage system and assessed its technical performance by using a PVsyst simulation. Specifically, this study was carried out to determine the optimal orientation and tilt angle of a solar panel for collecting maximum solar radiation. Borj Cedria, Tunisia, was taken as a case study site to investigate the optimum tilt angle using PVsyst and to estimate the global solar irradiance using the PV-GIS. The proposed system produced 1314 kWh of energy for the load, which is considered technically suitable for this area, thanks to the system's performance ratio of 58.3% and high specific efficiency generation, as well as a solar fraction of about 92.5%. From an economic point of view, the SAPS can save more than TND44,000 (12,991 Euros) per year from the purchase of the grid system's energy, and from the aspect of sustainability, 66.24 kg of CO<sub>2</sub> emissions annually can be avoided by utilizing the sun's energy. Furthermore, an efficient solar panel use requires its characteristics to be identified under various conditions. An original experimental setup was carried out in a photovoltaic laboratory to identify the photovoltaic characteristics of the SAPS. Experimental and simulation results performed using PSIM software were in good agreement, which showed the experimental setup's effectiveness.

**Keywords:** PV; system's site; optimum tilt angle; SAPS; PV-GIS site; PVsyst software; technical performance; experimental setup

**1. Introduction**

In Tunisia, the rural population occupies 33% of the total population, according to the UNESCO Institute of Statistics. The majority of the rural population is served by the electricity network, especially those living in high mountains or in remote areas. However, since 1998, Tunisia has not been able to produce sufficient oil and gas to meet its own growing demand for electricity. In addition, the implementation of a vast rural electrification program comes at a high cost.

To resolve this issue, many alternative solutions can be used. Using renewable energy systems is one of the optimal solutions. The growth of green power generation systems, such as photovoltaic systems (PVSs) and wind energy conversion systems, has exceeded the most optimistic estimations for supplying loads to rural and remote regions<sup>[1,2]</sup>. Tunisia is a country in northern Africa and borders the Mediterranean Sea, and this means that wind and solar energy systems would be very efficient in this part of the world.

Solar energy seems to constitute as one of the best alternative energy supply solutions. Nonetheless, an accurate PVS design is required to predict the photovoltaic (PV) characteristic curves under various meteorological conditions for a specific site. Therefore, to design a high-efficiency solar PVS, it is necessary

to study its optimal tilt angle and tilt position that are suitable for a given location. In order to maximize energy production from the received solar radiation, the angle of inclination must be set optimally during installation. Researchers have presented several methods to determine the optimum tilt angle and global solar radiation slope.

For example, Liu et al.<sup>[3]</sup> used a Hay model to calculate the optimum angle of inclination for a fixed grid-connected solar panel. A performance comparison of an optimized PV system and an actual PV system in the study by Mariano et al.<sup>[2]</sup> revealed a reduction of 9.4% in the electrical energy generated by the actual PV system in comparison with that by the optimized grid-connected PV system. Yang et al.<sup>[4]</sup> used computer-aided design (CAD) to calculate optimum PV parameters.

Yang et al.<sup>[5]</sup> and Sun et al.<sup>[6]</sup> discussed several methods to determine the optimum tilt angle and global solar radiation slope. Yang et al.<sup>[5]</sup> introduced the CAD method to identify the optimum tilt angle of a district's PVS. The study's derived equation can be used to provide a reference for the design of fixed photovoltaic power systems in China.

Li et al.<sup>[7]</sup> studied the amount of overall solar radiation and the optimum angle of inclination on inclined planes with several azimuths. The results showed that Hay's model was the best for the calculation of monthly average total radiation on inclined surfaces in Wuhan, China. At the optimum tilt installation angle, the total radiation increase was 4%, the PV power generation increase was 14.9%, and the performance ratio and the yearly power generation per watt were 86.1% and 1.02 kWh, respectively.

On the other hand, Wang and Shen<sup>[8]</sup> proposed the optimum inclination angle of solar components by taking resources into account.

The first objective of our study was to estimate the global solar irradiance throughout the year's seasons using the PV-GIS based on the latitude of a test site and the position of the sun during the considered days. The PVSyst software was then used to determine the optimal inclination angle and the global solar radiation slope.

PVSyst software presents a professional tool for dimensioning, performance analysis, and photovoltaic system study. This software was developed by Geneva University and has been used for simulating grid-connected, autonomous, and water-pumping systems<sup>[9,10]</sup>.

Several research studies that include off-grid or autonomous systems have used PVSyst to design and simulate processes. For example, Mansur et al.<sup>[11]</sup> analyzed the PVS performance for residential applications of an all-DC system. Another research by Mansur et al.<sup>[12]</sup> utilized PVSyst in a comparative study on PVSs for university buildings with different PV generator capacities.

Thus, the Photovoltaic Laboratory (LPV) at Borj Cedria Technopark, Borj Cedria, Tunisia, was chosen as a case study site to calculate the optimum inclination angle of a PVS. Long-term variations in global solar radiation during the year 2022 relating to this site and their impact on the optimum inclination angle were revealed to give guidelines for photovoltaic system design.

Among the LPV's activities is the development of nanomaterials for the production of photovoltaic cells. Therefore, it needed an experimental setup installed in the lab to identify the parameters of new solar PVSs.

Furthermore, an efficient solar panel use requires characteristics identification under various conditions in reference to temperature, solar radiation, etc.

In this context, this paper proposed an original test bench to measure the I–V and P–V characteristics of any photovoltaic module under diverse parameters, such as solar irradiance, temperature, and angle to incident light.

Several studies have addressed methods to measure the I–V characteristics of solar panels. Nalini et al.<sup>[13]</sup> and van Dyk et al.<sup>[14]</sup> discussed resistive load methods to create a variable impedance for I–V characteristic measurements, whereas in the study by Treble<sup>[15]</sup>, a capacitive load was investigated.

Benzagmont et al.<sup>[16]</sup>, Mahmoud<sup>[17]</sup>, Muñoz and Lorenzo<sup>[18]</sup>, and Spertino et al.<sup>[19]</sup> proposed a capacitor charging or discharging method to plot the I–V curve of PV modules.

The use of the one-device method can be found in the literature. For instance, Kuai and Yuvarajan<sup>[20]</sup> proposed the use of an electronic switch, such as a MOS transistor, while Meyer et al.<sup>[21]</sup> presented a power amplifier linked to a data acquisition board.

In this work, the I–V curves were acquired through a variable load (BK 8510 precision, 600W programmable DC electronic load) that supplied data ranging from open-circuit voltage to short-circuit current for each I–V curve.

Compared with these methods, our study aimed to provide a robust and very simple method based on real electrical measurements (I–V) and to compare the performance of the optimized PV system with that of a real PV system developed in our previous work<sup>[22]</sup>.

On the other side, the main principle of the methods cited above<sup>[13]</sup> was based on varying the impedance to extract current and voltage values, including short-circuit current and open-circuit voltage.

After that, we evaluated the validity of the results from the PV experimental setup by comparing with simulation results through the climatic information received from the Borj Cedria station.

Experimental and simulated results were analyzed and compared to illustrate the efficiency of the proposed experimental test bench.

## Study contributions

This study contributes the following:

- It assessed the off-grid PV energy configuration that can supply the expected load profile in the Borj Cedria area as a typical peri-urban site.
- It implemented a framework for a stand-alone photovoltaic system (SAPS) design and assessed its performance in a developing region.
- It provided a comprehensive feasibility study that considered technical, environmental, and economic aspects to determine the optimal and practical energy solution for the selected site.
- It can inform energy system planners, policymakers, energy investors, and other researchers on the technical, environmental, and economic conditions to electrify peri-urban areas using photovoltaic energy systems.

An overview of the paper is as follows: The SAPS configuration and the solar radiation model are presented in Section 2. In Section 3, with Borj Cedria as a study site, the optimum angle of inclination through the PVsyst software was calculated. The PV-GIS was utilized to estimate the overall solar irradiance based on the site's latitude and the sun's position. The assessment of the designed SAPS's technical performance is presented in Section 4. The new experimental setup is also explained in detail for solar panel parameters. Experimental results were analyzed based on this experimental test bench and compared with those of the simulation to illustrate the efficiency of the proposed experimental setup. This is followed by a discussion of

the results. Finally, Sections 5 and 6 conclude the study and provide policy recommendations, research limitations, and future research directions.

## 2. Laboratory PV system configuration

The SAPS configuration is depicted in **Figure 1**. It was installed in the LPV at Borj Cedria Technopark. It allows for the supply of residential loads to remote and off-grid regions. It consists of solar panels, a regulator, batteries, and a DC load. The photovoltaic system converts sunlight into direct electric current. The controller monitors the electrical input from the solar panels and controls the amount of battery charging and discharging. The surplus DC power is accumulated in the batteries when PV power is available. This stored energy may be consumed later when PV power is unavailable or the demand is high.

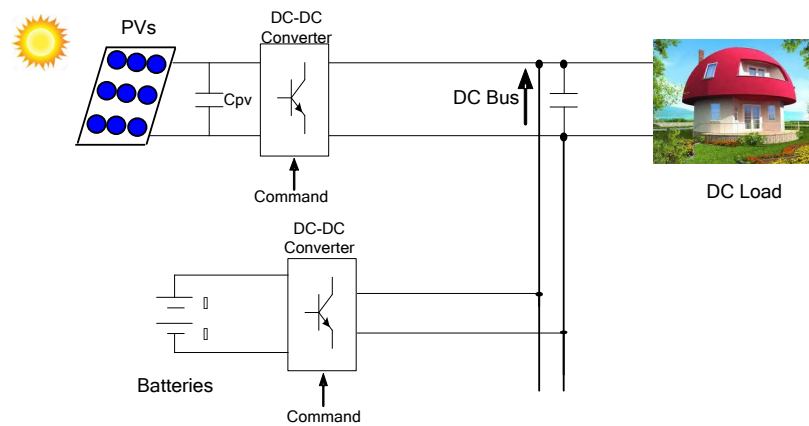


**Figure 1.** Stand-alone PV system.

## 3. Methodology and materials

### 3.1. Solar radiation modeling to install PV system

To determine solar radiation, it is necessary to know the angle of incidence,  $\theta_i$ , and the zenith angle,  $\theta_z$ , which depend on a site's geographical location, considering that the azimuth ( $\gamma$ ) and tilt ( $\beta$ ) angles are predefined. In **Figure 2**, the location of the site is assumed to be in the northern hemisphere and the panel is facing south<sup>[23,24]</sup>.

#### Solar geometry

Solar radiation forms an angle,  $\theta_i$ , with a normal solar panel; this angle is determined as described in Equation (1):

$$\cos(\theta_i) = \cos \theta_z \cos \beta + \sin \theta_z \sin \beta \cos(\gamma_z - \gamma) \quad (1)$$

where  $\gamma_z$  is an azimuth angle of the sun, while  $\phi$  and  $\delta$  are the site's latitude and the solar declination angle, respectively. The angle  $\theta_z$  can be written as Equation (2)<sup>[23–25]</sup>:

$$\cos(\theta_z) = \cos \phi \cos \delta \cos \omega + \sin \phi \sin \delta \quad (2)$$

The hour angle,  $\omega$ , is calculated by the following Equation (3)<sup>[23,24]</sup>:

$$\omega = 15 \times (12 - \text{solartime}) \quad (3)$$

Solar time is a calculation of the passage time according to the sun's position in the sky:

$$\text{solar time} = \text{standard time} + \frac{[4(L_{st} - L_{loc}) + E_T]}{60} \quad (4)$$

where  $L_{st}$ ,  $L_{loc}$ , and  $E_T$  are the standard longitude, local longitude, and time correction in minutes, respectively<sup>[26,27]</sup>.

### Extraterrestrial radiation ( $G_0$ )

The extraterrestrial radiation on a horizontal plane (using the site's longitude and latitude for a precise geographical location) in  $W/m^2$  is described by Equation (5)<sup>[23,24]</sup>:

$$G_0 = 1367 * (1 + 0.033 * \cos(\frac{360 * n}{365})) * \cos(\theta_z) \quad (5)$$

where  $n$  is the day number in the year, with  $n = 1$  for 1 January and  $n = 365$  for 31 December.

### Solar radiation on inclined panel

Usually, the available data on solar radiation are derived from measurements on a horizontal plane.

The total radiation,  $G_{tot}$ , received on an inclined photovoltaic panel is the sum of three components, which are diffused, direct, and reflected irradiances, as given by Equation (6) and illustrated in **Figure 2** and in the studies of Hailu and Fung<sup>[23]</sup>, and Bouabdallah et al.<sup>[24]</sup>.

$$G_{tot} = G_{dir} + G_{dif} + G_r \quad (6)$$

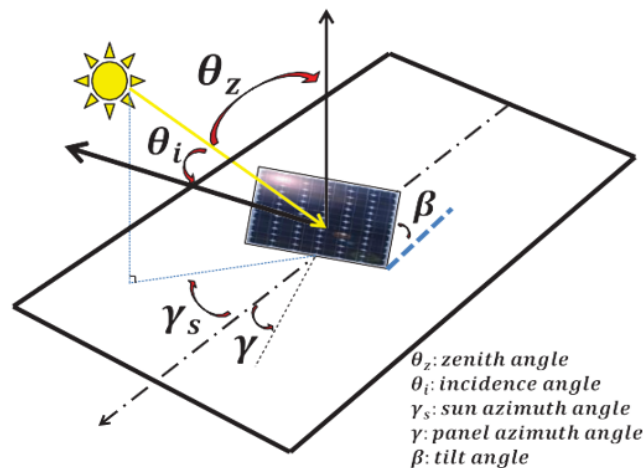


**Figure 2.** Solar angles for tilted solar panel<sup>[23]</sup>: slope, zenith, surface azimuth, and solar altitude angles.

## 3.2. Solar radiation: Orientation and tilt angle

### 3.2.1. Site assessment methodology

#### 1) Prepare appropriate site

The choice of an appropriate PV system site is a priority for the optimal exploitation of the solar resource. Several criteria must be satisfied to determine the optimum location of a PV system, such as the wide availability of solar radiation and the possibility of foreseeing its temporal and spatial distribution<sup>[25]</sup>.

Borj Cedria was taken as a case study site to perform our estimate of the PVS' potential (see **Figure 3**). Tunisia is a relatively small country in northern Africa, bordering the Mediterranean Sea. The Borj Cedria area is located in the northeast of Tunisia at  $36.71^\circ N$  latitude and  $10.42^\circ E$  longitude, according to the PV-GIS (see **Figure 4**).

This area receives a huge amount of solar radiation, according to PVsyst software (see **Figure 3**). Preliminary studies have shown that the site has huge energy potential.

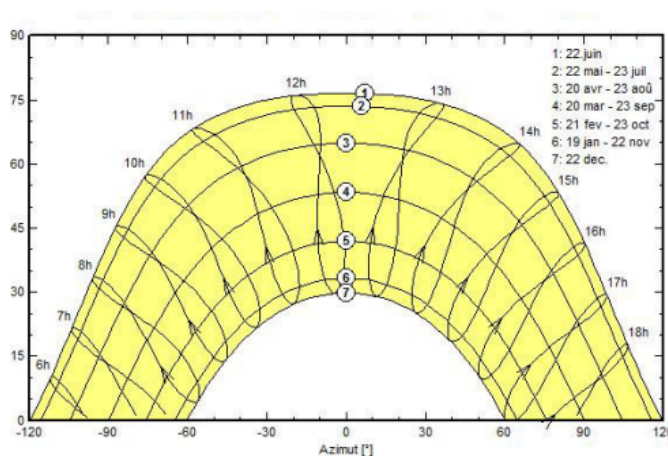


Figure 3. Sunshine over Borj Cedria area.

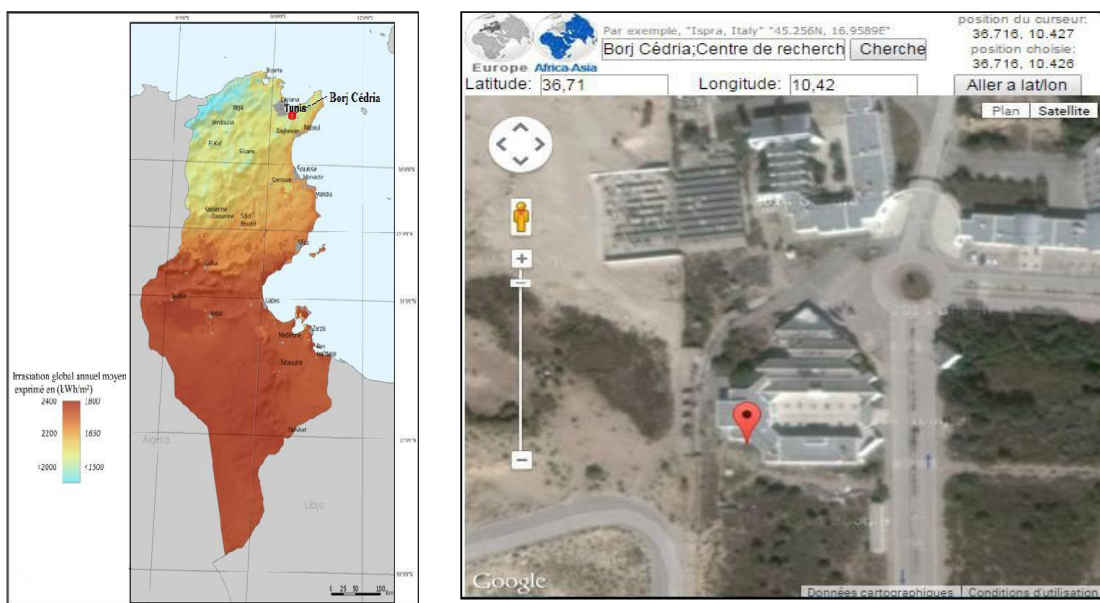


Figure 4. Borj Cedria’s site location from PV-GIS.

## 2) Prepare weather information site

To predict the PVS performance at a specific location, it was required to collect the climatic statistics for the area. In this study, meteorological data were collected from PV-GIS and Weather Underground websites.

The average monthly data of incident solar radiation on a horizontal surface and the temperature in the considered area are presented in **Figure 5**. It is shown that the incident solar energy is significant, particularly in the summer months, where it reached 8 kWh/m<sup>2</sup> per day. We noted that the month of July has significant global radiation and the month of August has an important average temperature of about 30 °C.

**Figure 5** also shows that even in winter, Borj Cedria enjoys one day of sunshine per month. The incident solar energy exceeded 2.5 kWh/m<sup>2</sup> per day in December and January.

The data collected from the PV-GIS were inserted in PVsyst (**Figure 6**) to carry out the next steps.

As a consequence, we predicted that any future PV system installed in the area could be extremely profitable (**Figure 3** and **Table 1**).

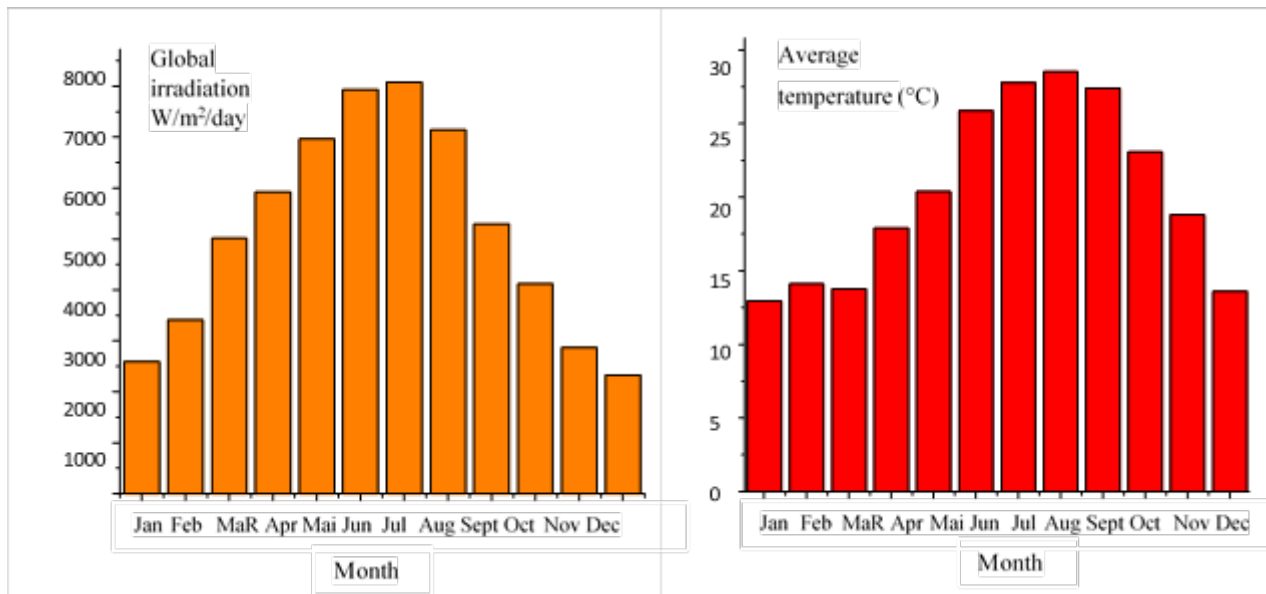


Figure 5. Monthly global radiation and temperature (°C) in 2022 for Borj Cedria site from PV-GIS and Weather Underground.

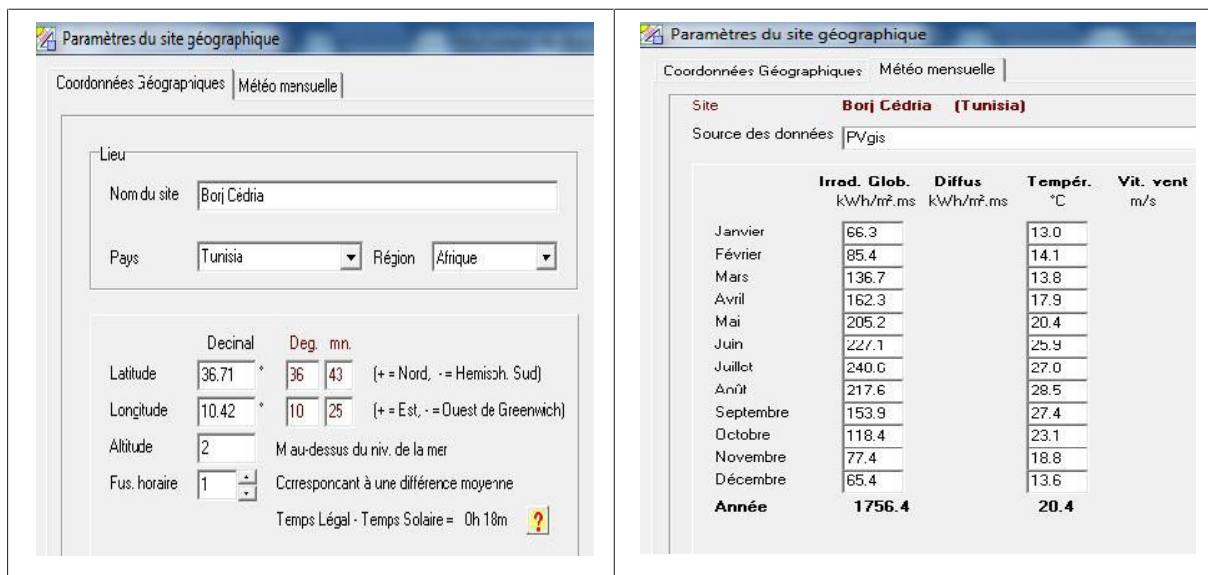


Figure 6. Geographical and meteorological coordinates' interface in PVsyst.

### 3.2.2. Optimal variation of tilt angle in Borj Cedria

Table 1 presents the data on global solar irradiance, direct horizontal irradiance, diffuse irradiance, and optimum inclination angle acquired from monthly measurements from the PV-GIS and PVsyst (Figure 6).

These data illustrated that the incident solar irradiance on a surface depended on its angle and orientation. For example, the solar irradiance data showed that the average global solar irradiance in July reached a maximum value of 8 kWh/m<sup>2</sup> per day. Furthermore, the maximum diffuse solar irradiance was 7 kWh/m<sup>2</sup> per day in the same month.

The optimal tilt angle at the Borj Cedria site varied between 3° and 63°: the highest optimum inclination angle was 63° in December and its minimum value was 3° in June, as shown in Table 1.

Therefore, the ratio of diffuse and global irradiances affected the optimal inclination angle and radiation slope, depending on the climatic condition.

**Table 1.** Monthly average global solar, direct, horizontal, diffuse irradiances, and temperature in 2022 at Borj Cedria site from PV-GIS and Weather Underground.

Month	H: Irradiation on horizontal plane (Wh/m <sup>2</sup> /day)	H <sub>T</sub> : Irradiation on plane with optimum inclination (Wh/m <sup>2</sup> /day)	Optimal inclination (degree)	Proportion between diffuse irradiation and global (D/G)	Average temperature (°C)
January	2590	4110	60	0.41	12.96
February	3410	4780	52	0.40	14.10
March	5010	6090	40	0.40	13.80
April	5920	6310	26	0.33	17.90
May	6960	6690	12	0.31	20.38
June	7930	7200	3	0.24	25.90
July	8080	7530	7	0.21	27.80
August	7140	7300	19	0.22	28.54
September	5290	6160	35	0.32	27.43
October	4120	5510	48	0.38	23.06
November	2870	4470	59	0.37	18.80
December	2330	3900	63	0.40	13.61
Year	5150	5840	35	0.31	-

In addition, for a surface at a specific place, the increase in its optimal angle results in the reception of more radiation during the winter than during the summer.

**Figure 7** presents the data for solar irradiation during 2022. It shows that the principal factors determining the slope of solar radiation are global solar, direct, and diffuse irradiances with respect to the horizontal plane.

For solar applications that require energy from solar panels mainly during the winter, the optimal angle should be large, whereas when the panels are used during the summer, the inclination should be small. For maximum energy availability during the entire year, the optimal tilt angle should be calculated.

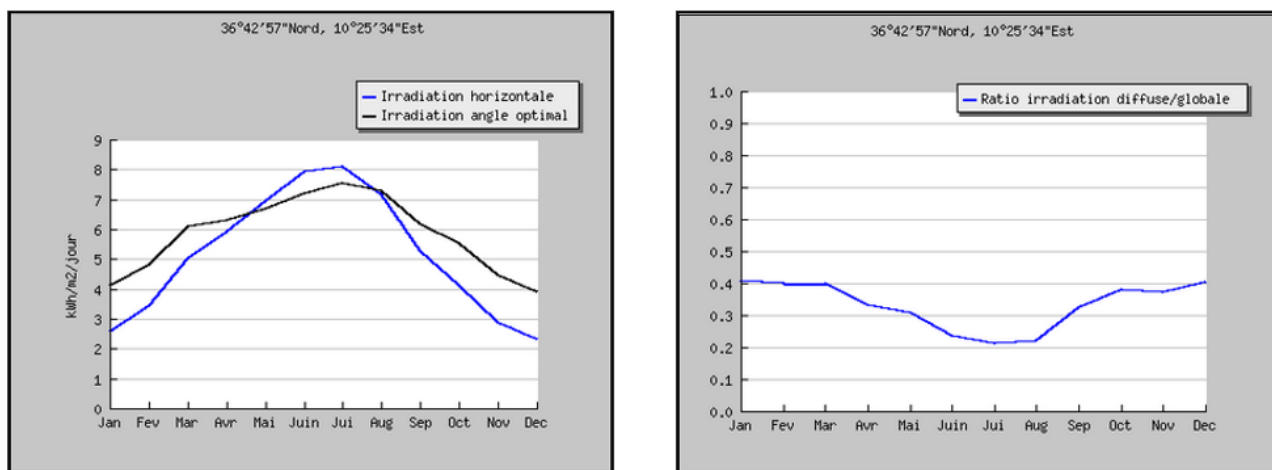


**Figure 7.** Solar energy simulation results: direct radiation and ratio of diffuse and global radiations.

### 3.2.3. Determination of optimal tilt angle

The tilt angle is defined as the module’s inclination angle measured with respect to the horizontal.



To maximize the overall solar irradiance received by a generator’s surface for one year, the optimal tilt angle should be maximized. Therefore, determining this optimum requires information on the annual global solar irradiance received at any angle between 0° (horizontal position) and 90° (vertical position) and the selection of the maximum power point.

Furthermore, different sites have different optimal angles for solar panels. To calculate the optimum inclination angle of the site under discussion, a simulation on PVsyst was made with the orientation and inclination of the PV panel (**Figure 8**).

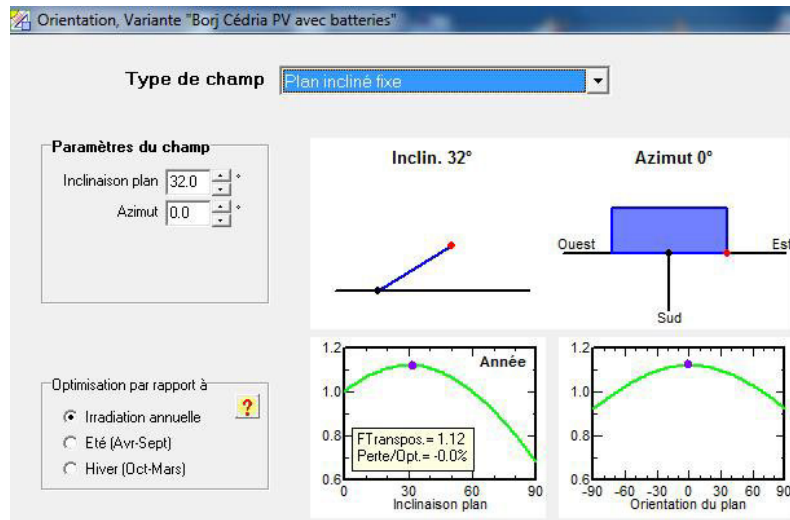


**Figure 8.** PV panel’s azimuth and tilt optimization from PV-GIS in PVsyst.

Since the considered area is situated at 36.71°N latitude and 10.42°E longitude, the simulation result showed that the PV panel’s orientation was to the south (azimuth of 0°) with an inclination of 32° so that the PVS would benefit from the maximum irradiation available during the period of use.

**3.3. Demand of electrical loads**

The SAPS in the remote laboratory in the region of Borj Cedria was supposed to be modest and not require huge amounts of electrical power devices. The daily electrical demand during a typical day for power loads composed of lighting (fluorescent lamps) is shown in **Figure 9** and **Table 2**.

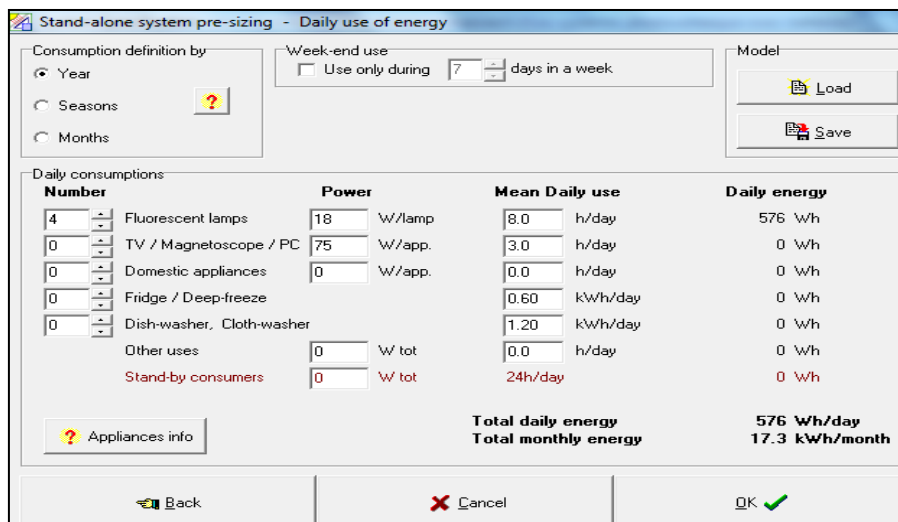


**Figure 9.** Daily average load demand in PVsyst.

Table 2. Laboratory load data from PVsyst.

DC load	No. of units used	Power/unit (W)	Functioning hours/day	Demand/day
Lights	4	18	8	576 Wh/day
Total				210,240 Wh/year

Estimating electrical needs involves calculating the daily electrical energy consumption of users. Thus, the electrical needs will be expressed in Wh per day (or kWh per day).

The daily average of load demand determined from PVsyst, as indicated in Figure 9 and Table 2, was 576 Wh per day. The estimated electricity consumption was 576 Wh per day at the Borj Cedria site.

### 3.4. PVsyst simulation

Figure 10 shows a typical layout of an off-grid PVS.

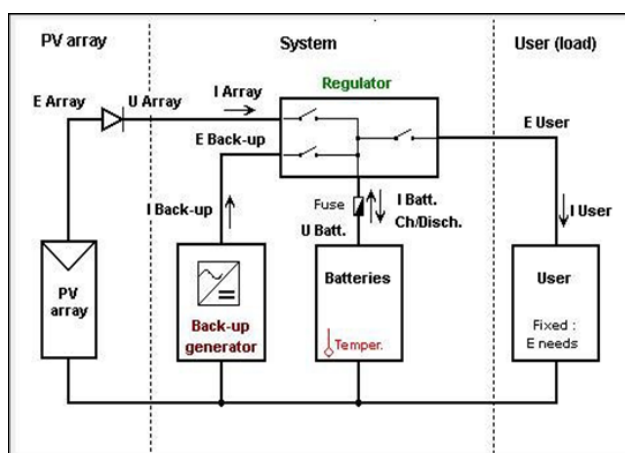


Figure 10. Typical layout of off-grid PVS.

## 4. Results and discussion

### 4.1. Experimental setup description

The experimental setup presented in Figure 11 was installed at the LPV, which is located at the Center for Research and Energy Technologies, Borj Cedria Technopark. The proposed system was carried out to identify the electrical characteristics of the solar cell, as well as those of the solar panel utilizing real data generated from the photovoltaic module. It can allow the supply of residential loads in remote and off-grid areas. Details describing the different instrument for the experimental test bench are presented in Figures 11–13.



Figure 11. Experimental setup at LPV.

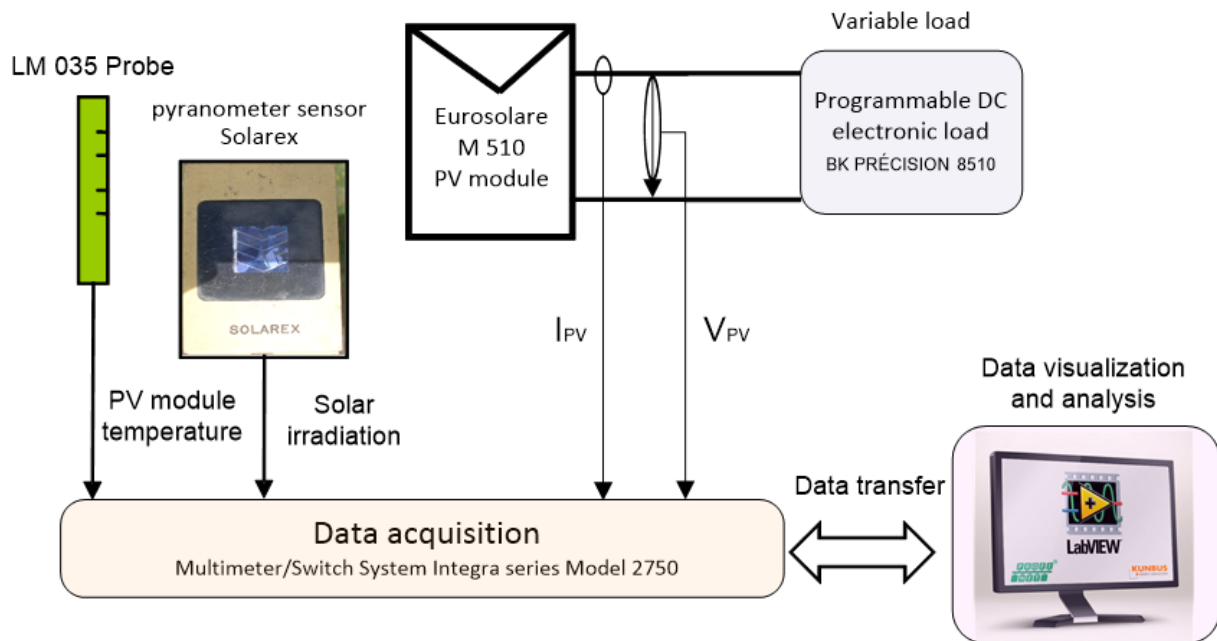


Figure 12. Experimental setup diagram.

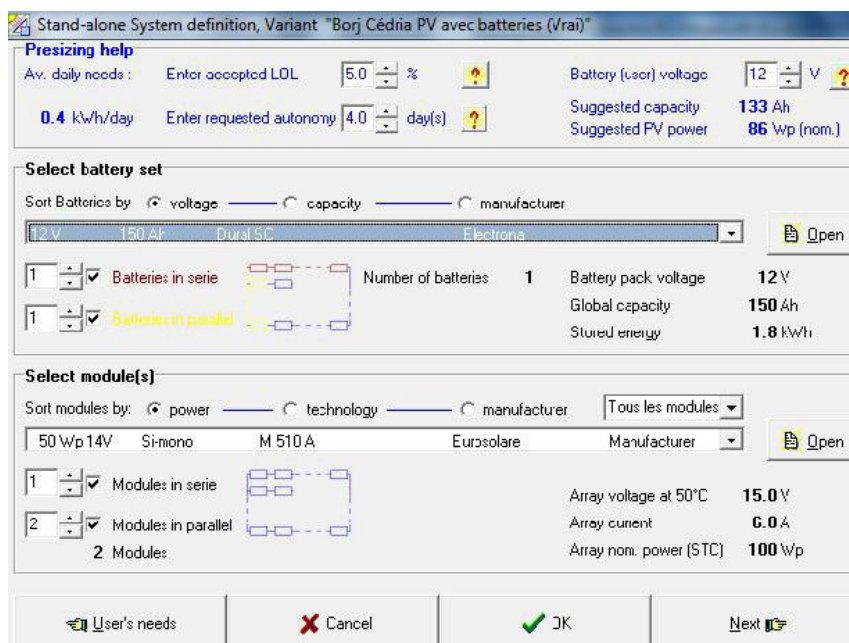


Figure 13. PVsyst interface for PV system sizing.

The evaluation of the proposed experimental setup was performed for a stand-alone PVS and contained the following main blocks (Figure 12): a PV generator (Eurosolare M 510 A), a pyranometer sensor (Solarex), a thermocouple (LM035 probe), a controller-charger, a battery, an acquisition chain (Multimeter/Switch System Integra series model 2750), an electronic load, and a computer.

The PV module was made up of monocrystalline solar cells. It was composed of 36 cells connected in series and gathered into four sub-strings of nine solar cells each. This module was equipped with four bypass diodes, each mounted in anti-parallel in order to protect the photovoltaic panel sub-strings.

The photovoltaic module was additionally interconnected to two parallel solar panels, as shown in the PVsyst interface (Figure 13), which supplied the same output voltage but at double the current.

The orientation of the PV panel installed in the LPV was to the south (azimuth of  $0^\circ$ ) with an inclination of  $32^\circ$ , as studied above.

Its major parameters are mentioned in **Table 3** under the standard test condition (STC) ( $1000 \text{ W/m}^2$ ,  $25^\circ\text{C}$ , light spectrum air mass of AM1.5) for the following electrical specification data:  $I_{SC}$  (short-circuit current),  $V_{OC}$  (open-circuit voltage),  $P_{MPP}$  (maximum power point),  $I_{MPP}$  (optimal current at maximum power point), and  $V_{MPP}$  (optimal voltage at maximum power point).

**Table 3.** Specifications of photovoltaic panel at STC ( $1000 \text{ W/m}^2$ ,  $25^\circ\text{C}$ ).

Parameter	Value
Maximum power	50 W
Optimal current	2.95 A
Optimal voltage	17 V
Short-circuit current	3.25 A
Open-circuit voltage	21.4 V

In this test, I–V curves were obtained using a variable load (BK precision 8510, 600W programmable DC electronic loads), which afforded data from  $V_{OC}$  to  $I_{SC}$  for each I–V curve sufficient to sweep the I–V curve of the module under study.

The pyranometer sensor served to measure the solar irradiance captured by the PV module surface. Then, the LM035 probe glued to the rear face of the PV module was employed to measure the temperature. The data acquisition system was equipped with a computer for data supervision and LabVIEW<sup>®</sup> for data visualization. Economical light sources, such as a 23-watt compact fluorescent lamp, were used as electrical loads.

A lead-acid battery was employed as the storage system to cover the shortfall of the PV generation system. The lead-acid battery's parameters are shown in **Table 4**.

**Table 4.** Lead-acid battery parameters.

Parameter	Value
$E_0$	12 V
$R_{bat}$	$0.153 \Omega$
$Q$	150 Ah

Note:  $E_0$ : battery constant voltage,  $Q$ : battery capacity, and  $R_{bat}$ : internal resistance

## 4.2. PVsyst simulation results

The technical performance assessment of the designed SAPS was performed through a PVsyst simulation. A result summary is shown in **Figures 14–16** and **Table 5**.

**Table 5** summarizes the performance of the SAPS. The global annual energy needed by users ( $E_{load}$ ) was 131.4 kWh, whereas the available solar energy ( $E_{avail}$ ) was 169.68 kWh per year. The quantity of energy that can be given to users was 121.58 kWh from the photovoltaic generator ( $E_{user}$ ). This energy gap was due to losses due to module temperature mismatch, solar irradiation availability, wiring loss, etc. On the other hand, the energy produced by photovoltaic generators was sufficient to supply the yearly load demand. The missing energy was highest in January, February, November, and December with a total of 9.824 kWh per year and the total unused energy was 37.69 kWh per year because of the full batteries.

Table 5. System performance summary.

Month	GlobHor (kWh/m <sup>2</sup> )	GlobEff (kWh/m <sup>2</sup> )	E <sub>avail</sub> (kWh)	E <sub>unused</sub> (kWh)	E <sub>miss</sub> (kWh)	E <sub>user</sub> (kWh)	E <sub>load</sub> (kWh)	SolFrac
January	80.3	119.2	8.76	0.005	2.676	8.48	11.16	0.760
February	95.5	124.6	9.24	0.008	2.052	8.03	10.08	0.796
March	155.3	182.9	15.52	3.360	0.000	11.16	11.16	1.000
April	177.6	180.1	15.68	3.876	0.000	10.80	10.80	1.000
May	215.8	197.3	17.43	5.091	0.000	11.16	11.16	1.000
June	237.9	206.3	18.64	6.647	0.000	10.80	10.80	1.000
July	250.5	221.5	19.64	7.196	0.000	11.16	11.16	1.000
August	221.3	215.9	19.21	6.824	0.000	11.16	11.16	1.000
September	158.7	177.8	14.87	3.049	0.000	10.8	10.8	1.000
October	127.7	164.4	13.16	1.489	0.000	11.16	11.16	1.000
November	86.1	124.2	9.3	0.149	0.403	10.40	10.80	0.963
December	72.2	111.3	8.23	0.005	4.692	6.47	11.16	0.580
Year	1878.9	2025.4	169.68	37.698	9.824	121.58	131.4	0.925

Note: GlobHor: horizontal global irradiation; GlobEff: effective global irradiation, corr. for IAM and shadings; E<sub>avail</sub>: available solar energy; E<sub>unused</sub>: unused energy (battery full); E<sub>miss</sub>: missing energy; E<sub>user</sub>: energy supplied to users; E<sub>load</sub>: energy need of users (load); SolFrac: solar fraction (E<sub>Used</sub>/E<sub>Load</sub>)

Figure 14 shows the analysis from the SAPS performance aspect of energy generation per installed capacity, which was normalized. The photovoltaic module’s daily energy loss was 1.07 kWh/kWp per day and the system’s daily energy loss was 0.29 kWh/kWp per day, whereas the unutilized energy was 1.03 kWh/kWp per day because of the full batteries. Moreover, the users received 3.33 kWh/kWp per day of energy, and the specific production yield (Y<sub>f</sub>) was 1215 kWh/kWp per year. As shown in Figure 15, the SAPS’s annual solar fraction was 92.5%, which would be adequate for a performance ratio of 58.3% per year.

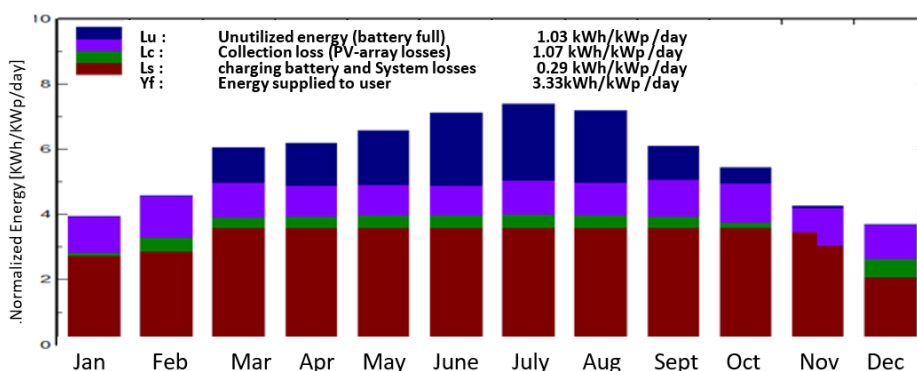


Figure 14. Normalized system production.

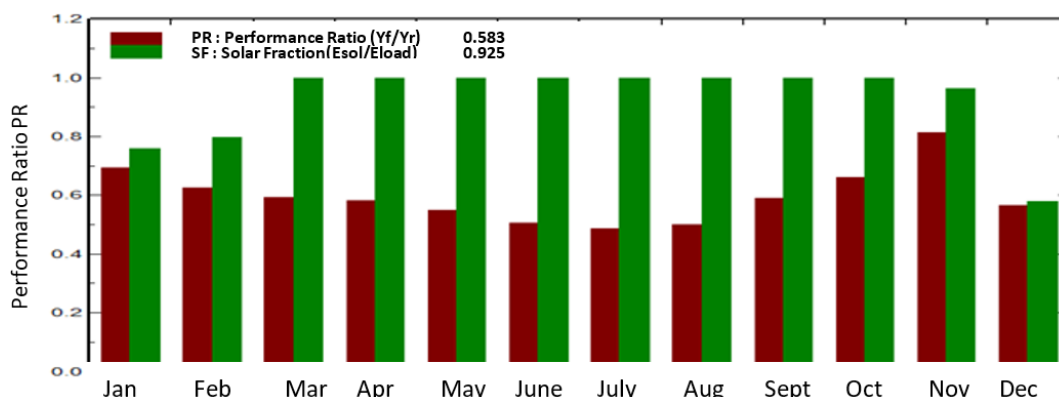


Figure 15. Performance ratio/solar fraction.

**Figure 16** illustrates the system’s annual energy loss. The power production at the STC of the photovoltaic generator was 203.2 kWh. Nevertheless, the total energy at the inverter output decreased to 164.125 kWh. The effective energy at the generator output was 132.0 kWh and decreased to 121.6 kWh due to battery and converter losses. Contributing factors to the energy generated from solar panels are as follows: radiance availability, module temperature mismatch, inverter conversion efficiency, and wiring losses.

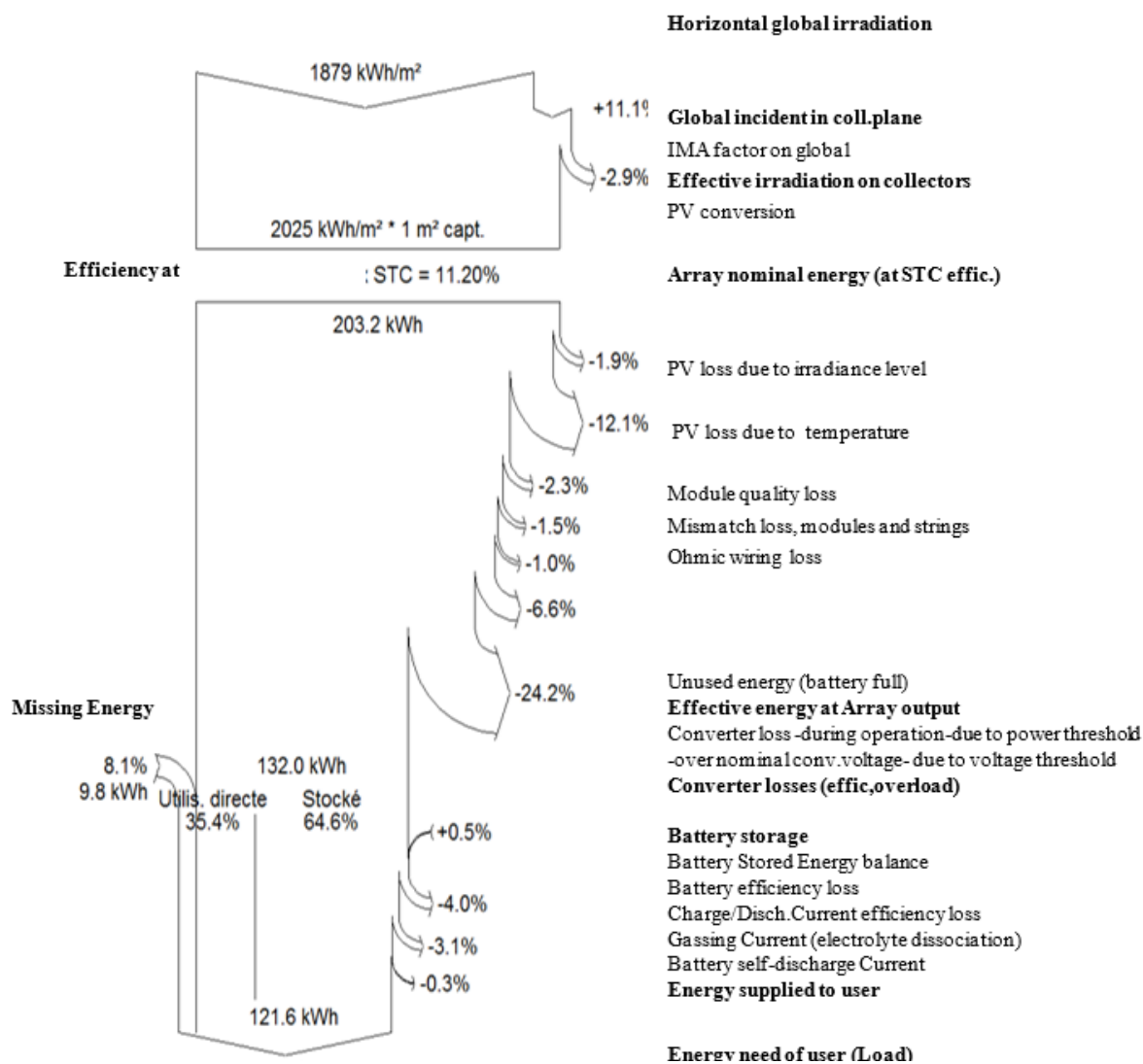


Figure 16. Loss diagram.

With reference to the SAPS’s economic aspect, the year-round load consumption was 131.4 kWh. As regards the Tunisian Company of Electricity and Gas (STEG), its tariff is TND0.338 per kWh.

As a result, the total cost savings from purchasing power from the grid system was TND44.413 per year. In terms of environmental sustainability, the 131.4 kWh of solar power generated annually is equivalent to more than 66.24 kg of CO<sub>2</sub> emissions per year avoided in the environment, at a rate of 0.46 kg of CO<sub>2</sub> emissions per kWh.

### 4.3. Experimental results

Experimental results were analyzed on the experimental test bench. **Figure 17** shows the characteristic current–voltage (I–V) and power–voltage (P–V) curves of the Eurosolare M 510 A panel at a temperature of 18 °C and incident solar irradiance from 437 W/m<sup>2</sup> to 1000 W/m<sup>2</sup>. It is obvious that the short-circuit current

of the solar panel depended on the insolation. It generated less current, and thus less power, when it received low radiance.

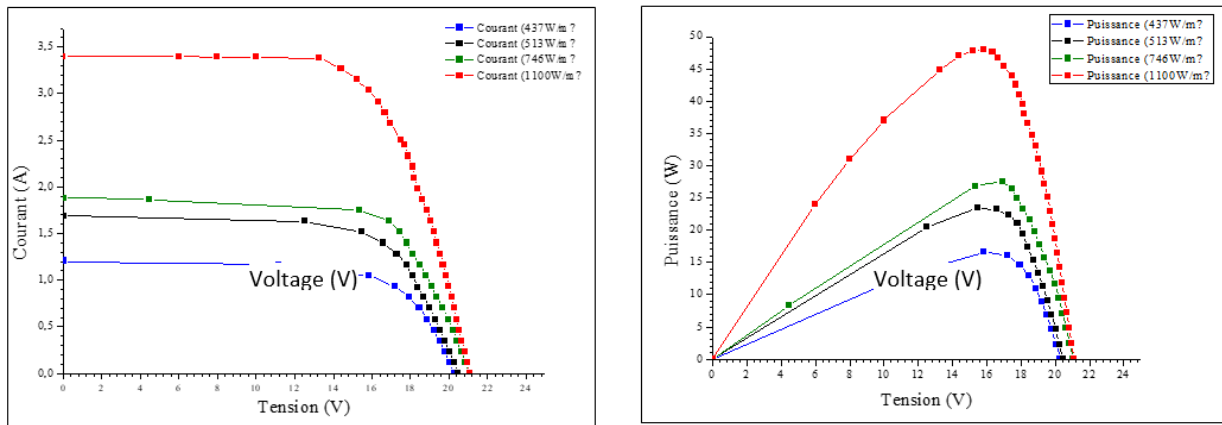


Figure 17. Experimental PV characteristics (I–V and P–V curves) at variable radiance.

The simulation results are shown in Figure 18 to compare with the experimental ones. It was found that experimental results were consistent with simulation results from PSIM software.

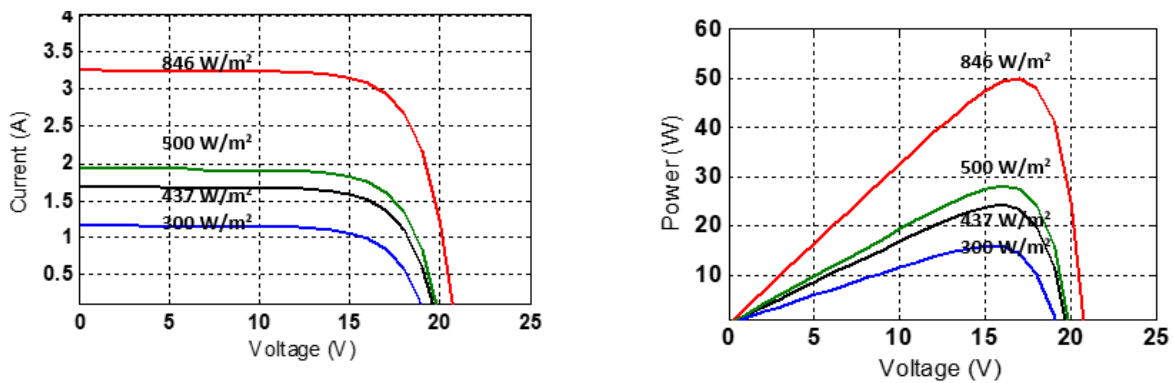


Figure 18. Simulated PV characteristics (I–V and P–V curves) at variable radiance.

The characteristics of the PV generator, composed of two Eurosolare M 510 A panels connected in parallel, were experimentally acquired, as illustrated in Figure 19. The analyses were supported by comparing the experimental results with those from the simulation performed in PSIM software (see Figure 20). Experimental I–V and P–V curves were measured three times, as shown in Table 6.

The measurements were carried out on three different days with variable conditions referring to solar radiation and temperature. It can be observed in Figure 20 that the PV generator’s open-circuit voltage depended on temperature. It generated less voltage when at a high temperature (30 °C). Increased temperature also meant higher stress on the panel, which decreased the open-circuit voltage by a factor of about two from 21.4 V at 18 °C to 19.8 V at 30 °C. It was found that the experimental results strongly agreed with the simulation results from PSIM software.

This test bench allowed us to compare this optimized PV system with a real PV system developed in our previous work<sup>[22]</sup>. It was shown that the electrical energy generation by the real PV system was 9% lower than that by the optimized SAPS. In fact, at 745 W/m<sup>2</sup>, the optimum PV system’s generated power was 41.5 W, while for the real PV system, the generated power was about 37.5 W<sup>[22]</sup>.

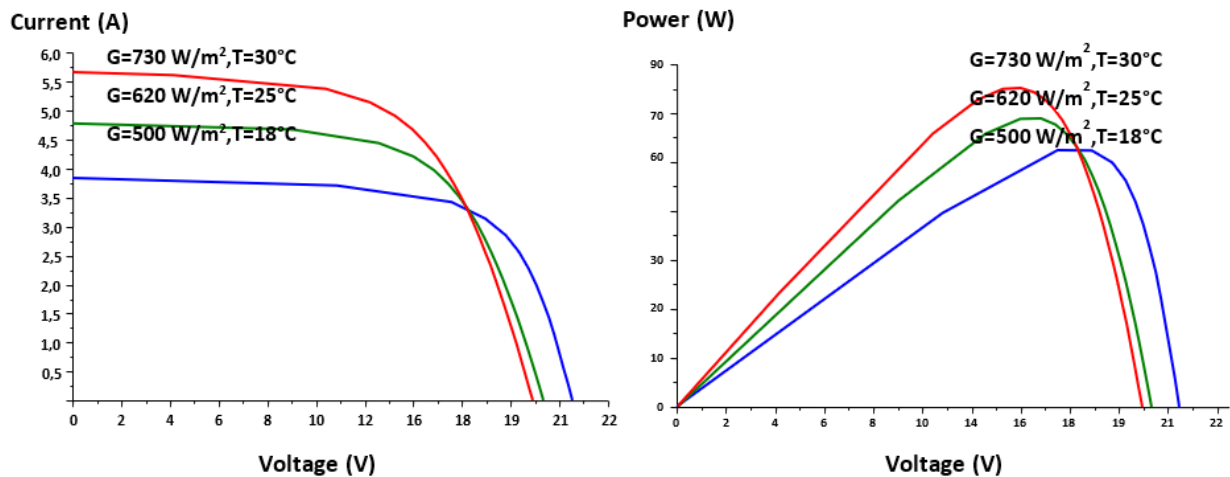


Figure 19. Experimental PV generator’s characteristics (I–V and P–V curves) as function of variable irradiation and temperature.

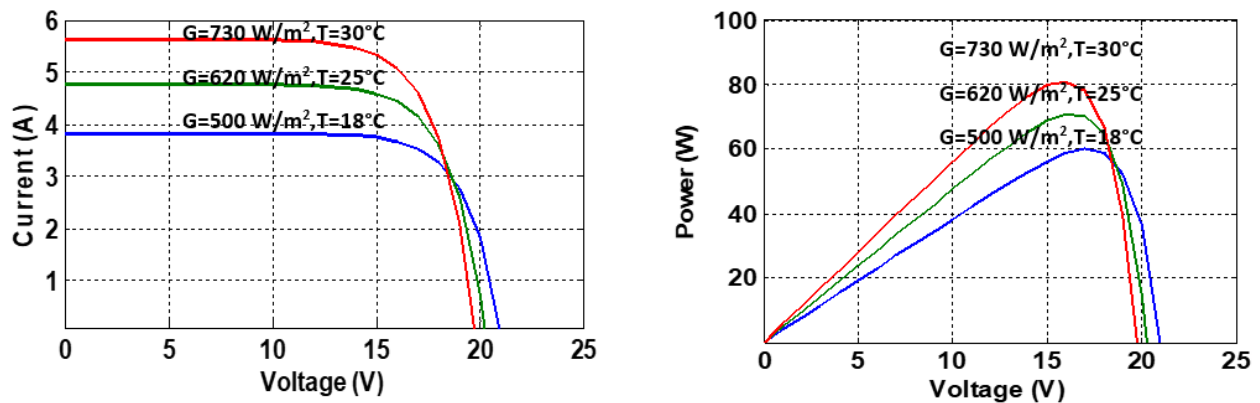


Figure 20. Simulated PV generator’s characteristics (I–V and P–V curves) as function of variable irradiation and temperature.

Table 6. I–V and P–V experimental tests.

Test 1	18 °C	500 W/m <sup>2</sup>
Test 2	25 °C	620 W/m <sup>2</sup>
Test 3	30 °C	730 W/m <sup>2</sup>

## 5. Policy recommendations, research limitations, and future research directions

The role of the Tunisian government is crucial in this respect.

The government should formulate a strong policy framework to reduce the dependence on conventional energy sources and to electrify pre-urban regions with off-grid solar PV systems, as Tunisia’s current economy is unable to afford the import of expensive thermal sources, especially oil.

Essential policy recommendations for all government agencies and stakeholders to benefit from this study are provided in the next subsection.

### 5.1. Policy recommendations

The following policy recommendations are suggested for the rapid deployment of SAPS electrification programs in Borj Cedria:



The study's results revealed that the region under discussion has huge solar energy potential for electricity generation. Hence, the related authorities should take the initiative and make effective strategies to initiate SAPS programs.

In addition, the geographical location of this region is technically and economically optimal for solar energy generation. Thus, the government should focus on this region on a priority basis.

Thus, it is advised that the government announce supportive policies for the maximum utilization of solar energy. The government should launch training programs and cultivate local professionals to manage, install, and operate solar PV systems.

## 5.2. Limitations and future research directions

The research also has some limitations. Only the region of Borj Cedria was considered. Therefore, the research findings are unsuitable for other regions of Tunisia. Future researchers can take a techno-economic and environmental feasibility analysis of SAPS power generation in other regions of the country. Moreover, researchers can consider developing a hybrid renewable energy system, such as wind and solar, in this area to make it independent of the national grid. Above all, the government's role is crucial to assist off-grid regions with such hybrid systems and overcome the energy gap in Tunisia.

In addition, this study used electricity supply and demand data on an average basis. Thus, it can be considered an essential future research direction.

## 6. Conclusion

An off-grid solar PV system has been identified as the best energy option to electrify the Borj Cedria region as a typical peri-urban site. Therefore, before installing a stand-alone photovoltaic system (SAPS) based on the battery storage system, it is essential to assess and analyze the techno-environmental and economic feasibility of this area.

A systematic method was developed to evaluate the solar PV potential of this selected area. Solar radiation received on a horizontal surface was examined first through the PV-GIS. Secondly, the optimum tilt angle was determined via PVSyst simulation to maximize solar energy output in this region.

The research results showed that this region has enormous solar energy potential and is suitable for electricity generation. By determining the optimum inclination angle, the energy output could be increased significantly.

A performance comparison between the optimized PV system and a real PV system developed in our previous work<sup>[22]</sup> was presented. It was revealed that there was a reduction of 9% in the electrical energy generation by the real SAPS in comparison with that by the optimized SAPS. In fact, at 745 W/m<sup>2</sup>, the optimized PV system generated power at 41.5 W, while the real PV system generated about 37.5 W<sup>[22]</sup>.

According to the simulation results, it was also found that the optimized system is technically adapted and suitable for the region thanks to its performance ratio of 58.3% per year and specific yield production of approximately 1215 kWh/kWp per year, in addition to its solar fraction of about 92.5%.

Also, this study revealed that 66.24 kg of CO<sub>2</sub> emissions could be mitigated annually by electrifying households with an off-grid solar PV system in the Borj Cedria region. In addition, from an economic point of view, the purchase of energy from the grid system can save more than TND44,000 (12,991 Euros) per year with the SAPS.

A sophisticated and low-cost experimental setup based on real electrical data was developed to identify the solar panel parameters and to compare the performance of this optimized PV system with that of a real PV system developed in our previous work.

The results of the PVS simulation carried out using PSIM software, which took into account the optimal inclination angle, agreed with the experimental data. This proved the efficiency of the proposed SAPS design.

Therefore, as a short-term prospect, the following will be necessary:

- To obtain a robust solar PV system, the photovoltaic panels must be supplemented by an inverter, which is used to supply AC loads (alternating current).
- For a more in-depth study on the costs associated with the PVS installation analyzed, future research should obtain the cost of the components of a photovoltaic system in Borj Cedria.

## Author contributions

Conceptualization, SS and WB; methodology, SM; Software, SS; validation, SS; formal analysis, SS, WB, SM, AJ and SEA; investigation, SS; resources, SS; data curation, SS; writing—original draft preparation, SS; writing—review and editing, SS and WB; visualization, SS; supervision, WB, SM and AJ; project administration, SM and AJ. All authors have read and agreed to the published version of the manuscript.

## Acknowledgments

This work was supported by the Tunisian Ministry of High Education and Research via Grant No. LESTE-ENIM-LR99ES31 under the India-Tunisia Cooperation project of HCHPS and LPV-CRTEEn-LR1OCRTEEnO1.

## Conflict of interest

The authors declare that they have no known competing financial interests or personal relationships that could have appeared to influence the work reported in this paper.

## References

1. Schmidt J, Cancellaa R, Pereira AO. An optimal mix of solar PV, wind and hydro power for a low-carbon electricity supply in Brazil. *Renewable Energy* 2016; 85(C): 137–147.
2. Mariano JDA, Campos HM, Tonin FS, et al. Performance of photovoltaic systems: Green office's case study approach. *International Journal of Energy and Environment* 2016; 7(2): 123–136.
3. Liu Z, Li Y, Xie J, et al. Optimum design for fixed grid connected photovoltaic array. *Journal of Yunnan Normal University (Natural Sciences Edition)* 2000; 20(6): 24–28.
4. Yang J, Mao J, Chen Z. Calculation of solar radiation on variously oriented tilted surface and optimum tilt angle. *Journal of Shanghai Jiao Tong University* 2002; 36(7): 1032–1036.
5. Yang G, Chen M, Chen Z. CAD method used in determining the optimum tilt angle of fixed PV arrays. *Acta Scientiarum Naturalium Universitatis Sunyatseni* 2008; 47(S2): 165–169.
6. Sun Y, Du X, Wang X, et al. Calculation of solar radiation and optimum tilted angle of fixed grid connected solar PV array. *Acta Energiae Solaris Sinica* 2009; 30(12): 1597–1601.
7. Li F, Zhao J, Duan S, et al. Evaluation of three models of monthly average total radiation on inclined surfaces and investigation of optimum tilt angle for array. *Acta Energiae Solaris Sinica* 2015; 36(2): 502–509.
8. Wang B, Shen Y. Discussion on the optimal tilt angle of solar installations from the perspective of resources. *Solar Energy* 2010; 159(7): 17–20.
9. Bouzguenda M, Al Omair A, Al Naeem A, et al. Design of an off-grid 2 kW solar PV system. In: Proceedings of the Ninth International Conference on Ecological Vehicles and Renewable Energies (EVER 2014); 25–27 March 2014; Monte-Carlo, Monaco. pp. 1–6.
10. Sharma V, Chandel SS. Performance analysis of a 190kWp grid interactive solar photovoltaic power plant in India. *Energy* 2013; 55: 476–485.

11. Mansur TMNT, Baharudin NH, Ali R. Performance analysis of self-consumed solar PV system for a fully DC residential house. *Indonesian Journal of Electrical Engineering and Computer Science* 2017; 8(2): 391–398. doi: 10.11591/ijeecs.v8.i2.pp391-398
12. Mansur TMNT, Baharudin NH, Ali R. A comparative study for different sizing of solar PV system under net energy metering scheme at university buildings. *Bulletin Electrical Engineering and Informatics* 2018; 7(3): 450–457. doi: 10.11591/eei.v7i3.1277
13. Nalini A, Sheeba PE, Rama ST, et al. Experimental setup for investigating the PV cells with distinctive aspects. In: *Proceedings of 2018 4th International Conference on Electrical Energy Systems (ICEES)*; 07-09 February 2018; Chennai, India. pp. 369–374. doi: 10.1109/ICEES.2018.8443192
14. Van Dyk EE, Gxasheka AR, Meyer EL. Monitoring current-voltage characteristics and energy output of silicon photovoltaic modules. *Renewable Energy* 2005; 30(3): 399–411. doi: 10.1016/j.renene.2004.04.016
15. Treble FC. On-site measurement of the performance of crystalline silicon PV arrays. *Renewable Energy* 1994; 5(1–4): 275–280.
16. Benzagmont A, Martire T, Beaufile G, et al. Measurement of the I(V) characteristics of photovoltaic array by the capacitive load method for fault detection. In: *Proceedings of 2018 IEEE International Conference on Industrial Technology (ICIT)*; 20–22 February 2018; Lyon, France. pp. 1031–1036. doi: 10.1109/ICIT.2018.8352320
17. Mahmoud MM. Transient analysis of a PV power generator charging a capacitor for measurement of the I–V characteristics. *Renewable Energy* 2006; 31: 2198–2206.
18. Muñoz J, Lorenzo E. Capacitive load based on IGBTs for on-site characterization of PV arrays. *Solar Energy* 2006; 80: 1489–1497.
19. Spertino F, Ahmad J, Ciocia A, et al. Capacitor charging method for I–V curve tracer and MPPT in photovoltaic systems. *Solar Energy* 2015; 119: 461–473.
20. Kuai Y, Yuvarajan S. An electronic load for testing photovoltaic panels. *Power Sources* 2006; 154: 308–313.
21. Meyer HS, de Souza Soares AM, de Araújo Neto OS, et al. An experimental setup to seek for maximum power point tracking of photovoltaic panels. *Academic Journals* 2013; 8(47): 2294–2297.
22. Slouma S, Baccar H. A control strategy for PV stand-alone applications. *Journal of Physics Conference Series* 2015; 596(1): 012010. doi: 10.1088/1742-6596/596/1/012010
23. Hailu G, Fung AS. Optimum tilt angle and orientation of photovoltaic thermal system for application in greater Toronto area, Canada. *Sustainability* 2019; 11(22): 6443. doi: 10.3390/su11226443
24. Bouabdallah A, Bourguet S, Olivier JC, Machmoum M. Photovoltaic energy for the fixed and tracking system based on the modeling of solar radiation. In: *IECON 2013 - 39th Annual Conference of the IEEE Industrial Electronics Society*; 10–13 November 2013; Vienna, Austria. pp. 1819–1824. doi: 10.1109/IECON.2013.6699408
25. Diop D, Drame MS, Diallo M, et al. Modelling of photovoltaic modules optical losses due to Saharan dust deposition in Dakar, Senegal, West Africa. *Smart Grid and Renewable Energy* 2020; 11(7): 89–102. doi: 10.4236/sgre.2020.117007
26. Vengatesh RP, Rajan SE. Investigation of cloudless solar radiation with PV module employing MATLAB–Simulink. *Solar Energy* 2011; 85(9): 1727–1734.
27. Iqbal M. *An Introduction to Solar Radiation*. Academic Press; 1983.